NUMERICAL MODELLING OF VELOCITY AND TEMPERATURE DISTRIBUTION INSIDE A CABINET DRYER ON NO LOAD

Olaoye, O.S[1*], Waheed, M.A[2] and Lucas, E.B[3]

[1,3] Mechanical Engineering Department, Ladoke Akintola University of Technology, P.M.B. 4000, Ogbomoso, Nigeria
[2] Mechanical Engineering Department, Federal University Agriculture, Abeokuta, Nigeria

* E-mail of the corresponding author: osolaoye@lautech.edu.ng

ABSTRACT: Majority of ginger farmers in Nigeria are using the open-sun drying method for drying agriculture produces. This method is time consuming and exposed the material to rain and contamination. A maintenance friendly and properly enclosed dryer is desired. A hybrid solar-biomass dryer was studied and adapted to suit the needs of small scale ginger farmers in Nigeria. The dryer model was evaluated using commercially available computational fluid dynamics (CFD) software to study natural convective heat transfer process inside the dryer. The results show that thermal heat distribution in the drying chamber was uniformly distributed for the natural convection model considered. Also, uniform heat distribution at the centre of the drying chamber is in the range of 335.0K to 353.0K which is sufficient for drying of ginger. The value of velocity across the plane is approximately the same as the velocity obtained through the experiment which was between 0.2 and 0.28 m/s. The flow velocity is high mainly along the axis of the hole from the base.

Keyword: Natural convection, Hybrid solar biomass, CFD, Numerical Simulation, Heat transfer, thermal distribution, Drying chamber, velocity.

1. INTRODUCTION

Preservation is always essential for all food crops ginger inclusive, so that they retain desired nutritional level, for as long as possible. Ginger, like other food crops, is, in the unprocessed form, largely perishable being susceptible to biologically and physically induced deterioration. Green [1] and Aworh and Egounlety [2] estimated food losses in developing countries as about 50% for fruits and vegetables and 25% for harvested food grain. Karim and Hawlader [3] and El-Sebaii & Shalaby [4] estimated wastage of fruits every year to be between 30-40%. These estimates show that every year, substantial quantities of food crops are lost through spoilage. Rahman [5] compiled several factors causing food crops spoilage. These include chemical and/or microbial activities. Microbial growth on food crops depends on initial condition of the crop as well as the condition of the environment wherein the food crops are stored. The commonly employed methods for food preservation are, freezing, vacuum packing, canning, preserving in syrup, food irradiation, addition of preservative chemicals, and dehydration/drying. According to Jangam and Mujumdar [6] drying is the most popular method of food preservation. Drying to a safe moisture content level hinders microbial growth within the stored material, although, several chemical and enzymatic changes do occur in food crops during processing and storage resulting in browning, heat damage and development of cracks from drying stresses induced as the surface dries faster than the core. Therefore, appropriate drying technique must be employed for proper drying of agricultural products. Sun drying has for long

been the traditional means of drying any agricultural crop (Sandeep, *et al.*, [7]). Sun drying takes relatively long duration. Crop temperature when drying in the sun ranges from 5 to 15^{o}C above ambient temperature. However, sun drying has some disadvantages which include inability to control the drying, insect infestation and microbial growth due to long period of drying (Ekechukwu and Norton [8]). To take care of the stated disadvantages sun drying has to be replaced by solar or artificial drying. Better understanding of the solar drying technique is needed to improve the quality of the product at minimal cost. Some of the factors influencing the rate of drying are the ambient temperature, velocity of air, direction of air movement, air relative humidity, and pressure on the material being dried. Drying rate also depends on the size and shape of the wet material (Forson *et al*.,[9]). Solar dryer can be categorized into natural convection and forced convection (Mohsin *et al*., [10] and Ghaffari and Mehdipour, [11]). These can be further divided into direct, indirect and mixed mode type. An inappropriate solar dryer may cause overheat or insufficient heat thus causing a quality deterioration of the dried crop.

Due to intermittent of sun there is need for additional supply of heat when there is no sun so that there will be continuous drying. The type of dryer that can do this kind of work is the hybrid dryer. The hybrid dryer has additional source of heat which is charcoal (Prasad and Vijay [12]).

The prediction of the airflow and temperature inside the dryer helps to design most suitable geometrical configurations of the device and improving the drying process. Computational fluid dynamics (CFD) can be used for the analysis and investigation of air flow rate, temperature distribution pattern inside the solar dryer through appropriate simulation of energy and momentum equations (Singh Chauhan *et al*., [13]). Numerical techniques have been used to model the behaviour of the airflow inside several kinds of dryer (Rigit and Low [14], Dyah *et al*. [15], Mathioulakis *et al*.[16] Maia *et al*., [17]).

The present paper presents the numerical simulation of the airflow inside a hybrid solar-biomass dryer, performed with the Autodesk simulation CFD code. The numerical results of velocity and temperature of the airflow were compared with the experimental data obtained.

2. EXPERIMENTAL SET UP

A hybrid solar- biomass dryer was designed, constructed and tested in Ogbomoso (Nigeria). The solar dryer consists of transparent single glazing (2 mm thickness), four drying trays of perforated wire mesh base (area 0.192 m^2), three adjustable vents (0.66 x 0.08 m^2) which serve as a chimney to prevent condensation. The single glass inclined at 18.13^{o} according to Ogbomoso Latitude (8.13^{o}) and it has a metallic frame (for rigidity) in which all the sides are wood to prevent heat loss. In between the inner plate and outer wood is fiber glass an insulator that helps in reducing further heat loss. The angle of inclination should be 10^{o} more than the local geographical latitude for best all year performance (Bolaji [18]). There is a door at the side of the dryer for easy feeding and removal of drying material. The capacity of the dryer is 3 kg. The openings at the base of the dryer are to allow hot air in when using biomass. The solar collector has three openings at the top and four opening at the bottom for air going in and out easily. The characteristic of the cover plate has to be able to transmit maximum solar energy to the absorbing plate, minimize heat loss from the absorbing plate to environment and to shield the absorber plate.

2.1 Charcoal Fueled Stove Dimensions

Charcoal stove is to provide indirect heating to the dryer and its temperature could be controlled by maintaining the combustion in the stove with opening or closing of the primary air supply. The charcoal stove dimensions are 0.61 m x 0.66 m x 0.58 m surrounded by brick walls (0.70 m x 0.75 m x 0.67 m). A burner grate with a perforated tray is provided inside the stove. The exhaust gases exit via a 7.5 cm diameter and 70 cm long chimney located at one side of the stove. To lengthen the flow path of exhaust gases and maximize the transfer of heat to the stove walls, three metal baffle plates are inserted at a distance of 0.1 m above the grate and below the chimney in the burning chamber. The brick chamber has 13 rectangular holes for fresh air entry and one biomass feeding hole having dimension of 0.018 and 0.011 m^2**,** respectively. To prevent excessive temperature in the drying cabinet, an insulated layer is placed in between the solar dryer and biomass stove that is also act as a thermal device.

2.3 Mathematical Model

The modelling of temperature and velocity distributions inside the dryer was performed by utilizing commercially available computational fluid dynamics (CFD) software Autodesk (2012) that includes a solver based on finite element method for structured and unstructured grids. The modelling was performed on an empty chamber without ginger.

The mass, momentum and energy conservation equations are given in a general form by:

$$\frac{\partial \rho}{\partial t}+\frac{\partial(\rho u)}{\partial x}+\frac{\partial(\rho v)}{\partial y}+\frac{\partial(\rho w)}{\partial z}=0$$

$$\rho\frac{\partial u}{\partial t}+u\frac{\partial(\rho u)}{\partial x}+v\frac{\partial(\rho v)}{\partial y}+w\frac{\partial(\rho w)}{\partial z}=\rho g_x-\frac{\partial p}{\partial x}+\frac{\partial}{\partial x}\left[2\mu\frac{\partial u}{\partial x}\right]+\frac{\partial}{\partial y}\left[\mu\left(\frac{\partial u}{\partial y}+\frac{\partial v}{\partial x}\right)\right]+\frac{\partial}{\partial z}\left[\mu\left(\frac{\partial u}{\partial z}+\frac{\partial w}{\partial x}\right)\right]+S_w+S_{DR}$$

$$\rho C_p\frac{\partial T}{\partial t}+\rho C_p u\frac{\partial T}{\partial x}+\rho C_p v\frac{\partial T}{\partial y}+\rho C_p w\frac{\partial T}{\partial z}=\frac{\partial}{\partial x}\left[k\frac{\partial T}{\partial x}\right]+\frac{\partial}{\partial y}\left[k\frac{\partial T}{\partial y}\right]+\frac{\partial}{\partial z}\left[k\frac{\partial T}{\partial z}\right]+q_V$$

$$\left(u\frac{\partial(\rho T)}{\partial x}+v\frac{\partial(\rho T)}{\partial y}\right)=\frac{\kappa}{c_p}\left(\frac{\partial^2 u}{\partial x^2}+\frac{\partial^2 u}{\partial y^2}\right)$$

The two source terms in the momentum equations are for rotating coordinates and distributed resistances respectively. The distributed resistance term can be written in general as (Autodesk, [19]):

$$S_{DR}=\left(K_i+\frac{f}{D_H}\right)\frac{\rho V_i^2}{2}-C\mu V_i$$

The other source term is for rotating flow, this can be written as:

$$S_\omega=-2\rho\omega_i\times V_i-\rho\omega_i\times\omega_i\times r_i$$

Where i refers to the global coordinate direction and r is the distance from the axis of rotation

$$P = P_{ref} + \rho_{\infty} g_i x_i + P^*$$

Where P_{ref} is reference pressure, ρ_{∞} is reference density, g_i gravitational vector, x_i is the distance vector from origin and P* is the dependent variable.

The numerical solution of the above equations involves the use of specific boundary conditions, in particular at surfaces bounding the domain. In this study the boundary conditions were defined as function of the experimental data as following:

Boundary conditions: Total heat generation of 2000 W from bottom (assumed), velocity of 0.68 m/s flows through all the four inlet space at the base (assumed), a gauge pressure of 0 Pa at the three exit space at the top was assumed.

Initial condition: it was assumed that velocity was 0 m/s at the initial state

The flow is simulated considering a steady state operating condition. The air inside the dryer was assumed as an ideal gas, with an ambient pressure of 92.000 Pa. This is a characteristic ambient pressure value for Ogbomoso, where the dryer was installed.

3. RESULTS AND DISCUSSION

The prototype of the hybrid solar dryer was experimentally tested without the trays and with no load. The airflow velocity and temperature were measured in the dryer outlet. The ambient temperatures and the wall temperatures of the dryer were also measured. The ambient temperature was 305±2.0 K. At the time the test was performed, the measured time average temperature of the wall drying chamber was 314±2.0 K, of the solar absorber was 318±2.0 K, and the outlet average temperature of the air was 311.0±2.0K. The mass flow rate calculated at the outlet of the dryer was 0.0150±0.0005 kg/s.

The airflow inside the hybrid solar-dryer was simulated using Autodesk software package. The employed computational domain includes the dryer without the trays and without the drying products. The total number of elements and nodes varied among the different simulations and was in the range 138816 elements and 34784 nodes respectively. The mesh (figure) in regions near the walls was refined using the inflated boundary conditions tools of Autodesk.

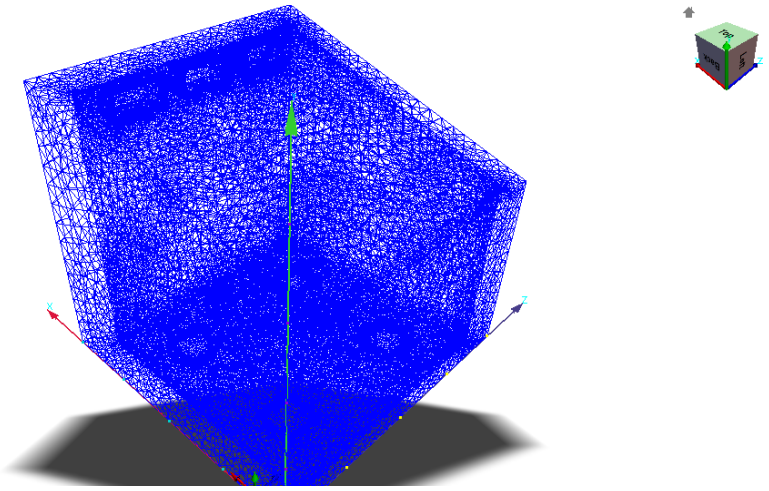

Figure 1: Surface Mesh of the Dryer

3.1 Simulation of Dryer with Biomass Mode

Figure 2 shows ambient airflow into the dryer through the four openings at the base of the solar dryer. It can be seen that the distribution of temperatures inside the dryer in the vertical plane is not homogeneous, with high velocity along the four opening vertical upward but other places inside these section are homogeneous. The reason for this is that air enters through these opening and because there are no trays inside, the air just flows upward. The velocity distribution along the plane as shown in figure 2a varies between 0 and 0.25m/s, while the distribution along the axis of opening from base varies from 0.3 and 0.5 m/s *(between 0.5 and 0.75 m/s)*. The maximum velocity that can be achieved across the plane apart from path along the hole is 0.26m/s and it is found to be concentrated at small path in the middle of the collector.

The velocity increases as it flows across the drying chamber and out through the chimney. From the simulation results, the mean velocity of air escaping from chimney is 0.75m/s. The value of velocity across the plane is approximately the same as the velocity obtained through the experiment which was between 0.2 and 0.28m/s. Observation of the velocity distribution indicted that the flow velocity in the solar dryer is not uniform. The flow velocity is high mainly along axis of the hole.

Figure 3 – flow streamlines along solar and drying chamber- shows the hottest air coming from the solar collector bottom wall from a recirculation region in the drying chamber vertical direction, flowing first near the drying chamber backward wall, and then turning around the other wall of the drying chamber. In the average the flow behaviour above described seems to be the main flow pattern in the drying chamber section. As expected, this recirculation region is formed by the buoyancy. This flow pattern indicates that the region near backward wall should be the more effective for drying chamber.

Figure 4- velocity inside a middle plane dryer- the velocity increases towards the exit section. This behaviour was expected, since the flow cross-section decreases in this direction. It can also be noticed that the velocity is homogeneous in a vertical plane in the solar collector and drying chamber, denoting a small turbulent. Reynolds number flow in almost all the drying section (approximately 9 X 10^3). This behaviour of the temperature and velocity is desirable for drying purposes, since it guarantees a high-quality and homogeneous drying process.

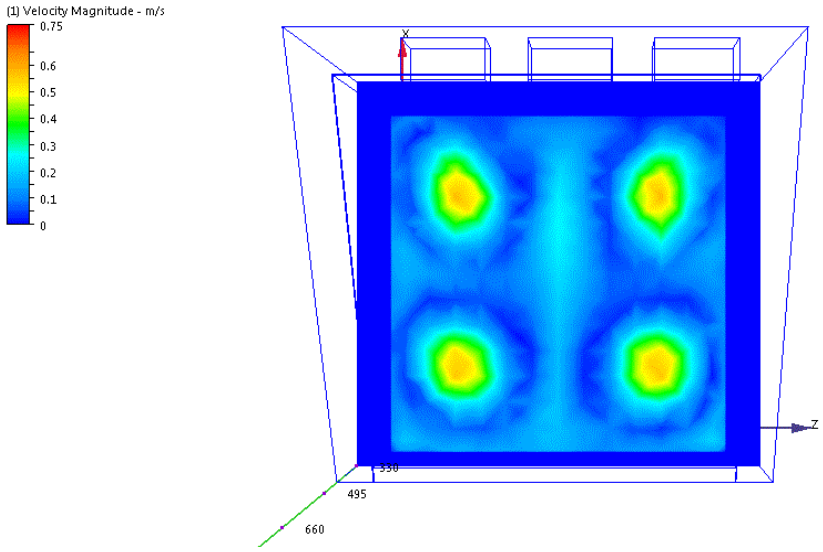

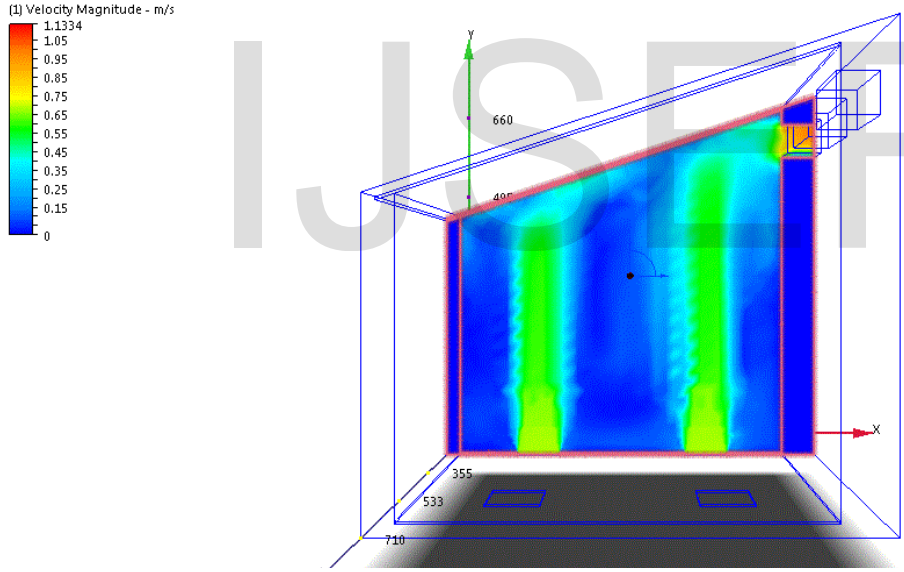

Figure 2: Velocity Vector of Fluid flow under Biomass Mode
NB: x axis is horizontal; y axis is vertical and z axis is the thickness

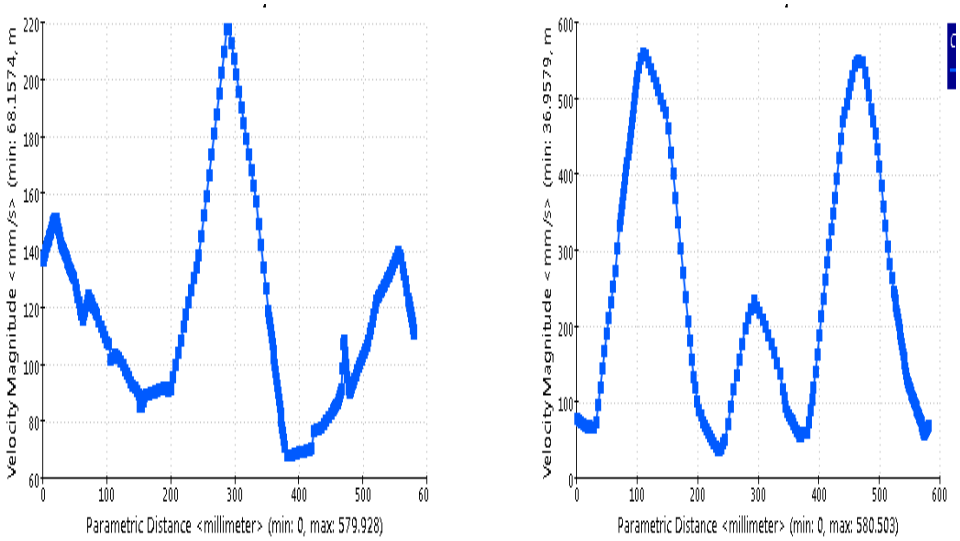

Figure 3: Velocity Vector of Fluid flow under Biomass Mode

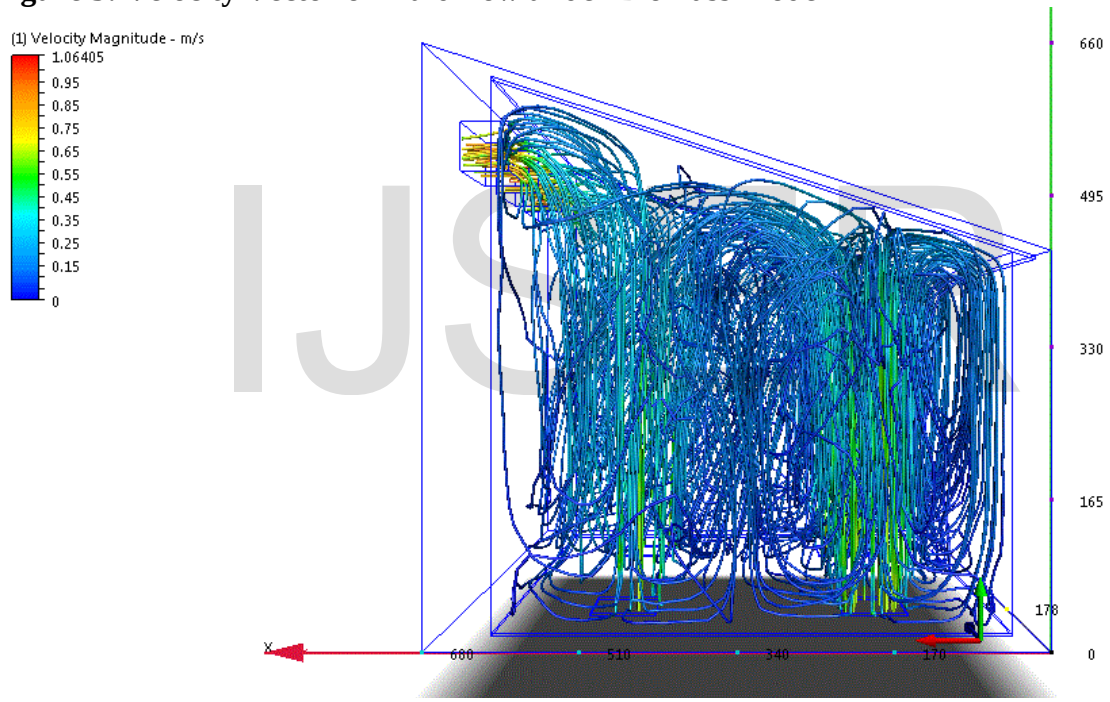

Figure 4: Streamline of air Flow in the Dryer.

3.2 Simulation Temperature Distribution

Figure 5 shows the temperature distribution inside the solar-biomass dryer. Figure 5a shows the graph of temperature distribution along the vertical section of the dryer and showing the temperature distribution across the air inlet of the dryer. It was observed that the highest temperature is concentrated around the absorber plate and has the temperature range between 338K (65^{o}C) and 368K (95^{o}C). Also the level where the fourth and third trays are located in the dryer gave the temperature of 328K (55^{o}C) and 326K (53^{o}C). Figure 5b shows that there is other place, the reason being that air will carry the temperature and there will be temperature variation as it moves. The temperature decreases as it moves up, this may be as a result of heat loss. The temperature on the solar chamber walls increases towards the drying chamber.

From Figure 5(a) temperature variation along the vertical axis of the dryer show that (for heated surface from bottom) temperature is higher in the lower plate because it was close to the source of heat, there is good temperature distribution along the height that ranges from 328K (55^{o}C) at 500mm and 324K (51^{o}C) at 400 mm which is in close agreement with the experimental results. Figure 5(b) shows that there is lower temperature along the axis of air flow this is due to constant air flow that carries the heat at high rate.

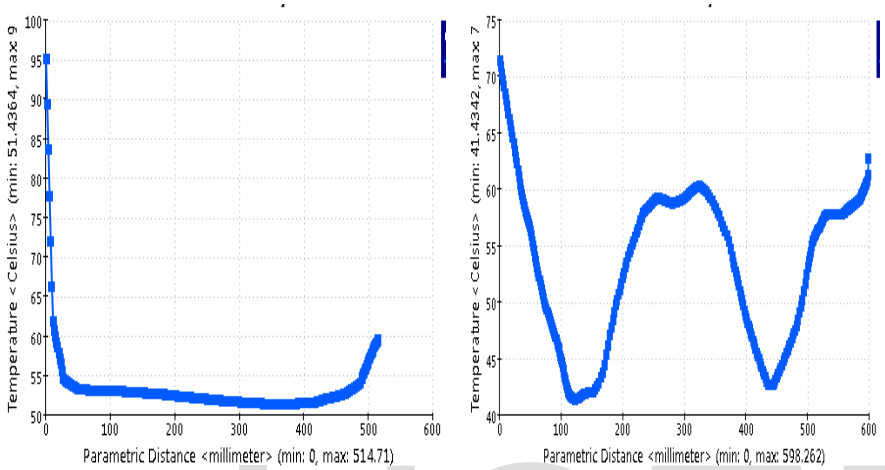

Figure 5: (a) Temperature Distribution along the Vertical axis (b) Temperature Distribution across the inlet

Figure 6(a) shows the temperature across the x – y plane, the edges has highest temperature, this is due to conduction by the internal metal plates and temperature across the plane is between 328K (55^{o}C) and 343K (70^{o}C). Figure 6(b) represents the air flow temperature in a plane situated in the middle of the dryer (inlet section, drying chamber and exit region). It can be seen that temperatures distribution inside the dryer in this vertical plane is almost homogeneous, except in the bottom and walls, where higher temperatures are obtained, of about 368K (95^{o}C) as well as the highest temperature gradients. Overall, the mean temperature gradient between the dryer inlet and out let regions is approximately equal to 368K (95^{o}C) and 324K (51^{o}C) which is a reasonable value.

Figure 7 shows temperature distribution in several horizontal planes inside the drying chamber. In these cases it is observed a uniform cross sectional distribution of the temperature field inside the drying chamber. In fact the temperature changes more along and across the bottom plate than along and across the drying chamber. This temperature distribution is beneficial, because it is expected a uniform drying process in order to avoid different final moisture content of the products. Trays and the drying products were not considered in the simulation leading to more uniform temperature distributions.

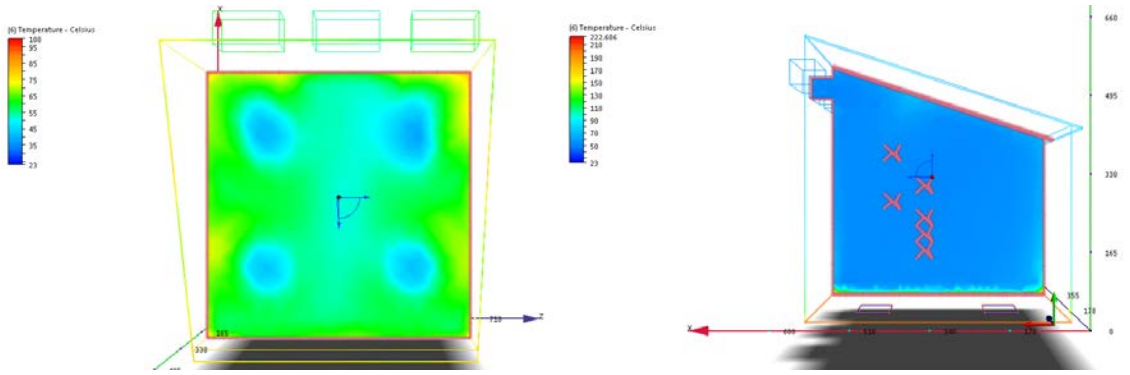

Figure 6: Temperature Distribution Across the x – y Plane (b) Along the vertical axis

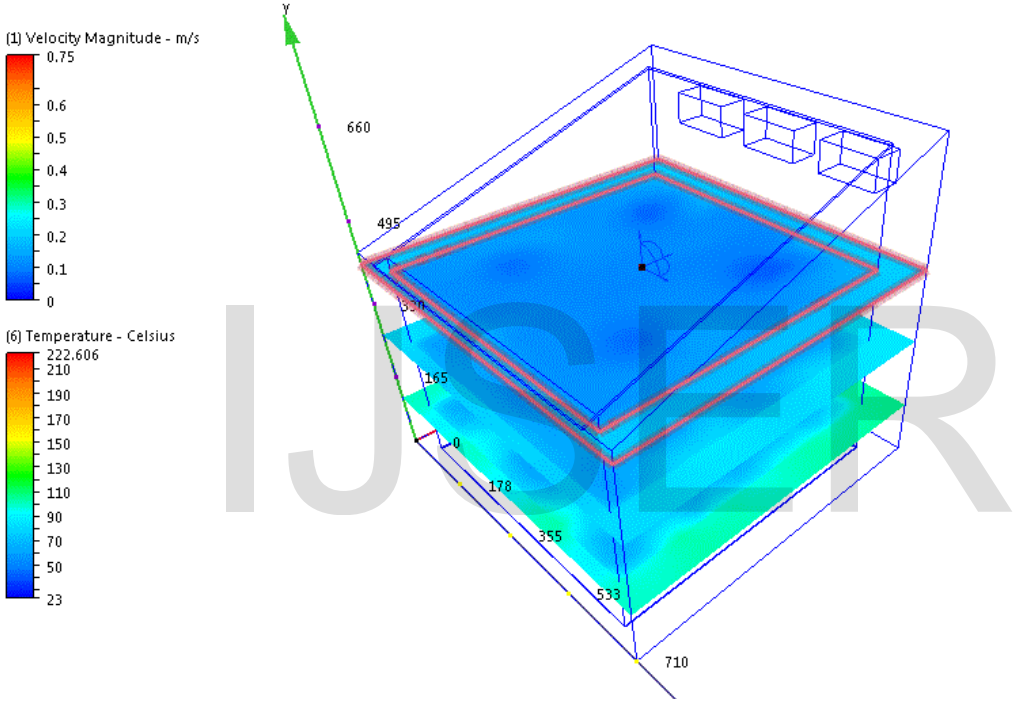

Figure 7: Temperature Distribution along Horizontal Plane

3.3 Simulation of Dryer under Solar Mode

Initial simulation was done on when additional heat source is needed to augment solar energy for continuous drying process.

The figures 8 – 10 show the simulation under solar mode for different time of the day to ascertain the time that biomass is needed.

The temperature distribution under solar mode shows that adequate drying can be done between 9am and 6pm without biomass backup, provided that there is no cloud. However, from 6pm, the temperature distribution in the dryer reduces below adequate temperature which is an indication that there must be another heat source for continuous drying. The maximum temperature for 7pm is about 312K (39^oC) and that of 7am is about 300K (27^oC). The temperatures attained at this two periods are inadequate for proper drying; therefore, biomass heat source is needed for proper drying to take place. The results got are in close agreement with

the experimental results. Therefore, hybrid dryer is the most appropriate dryer for continuous drying applications.

The simulation results were validated by comparing with the results obtained from experiment measurements. Hybrid mode is the most appropriate mode for drying application since it provides the highest temperature and falls within the required drying temperature range. The low temperature spot (which is spot along the hole from bottom) was identified and will be assisted in the improvement of dryer design.

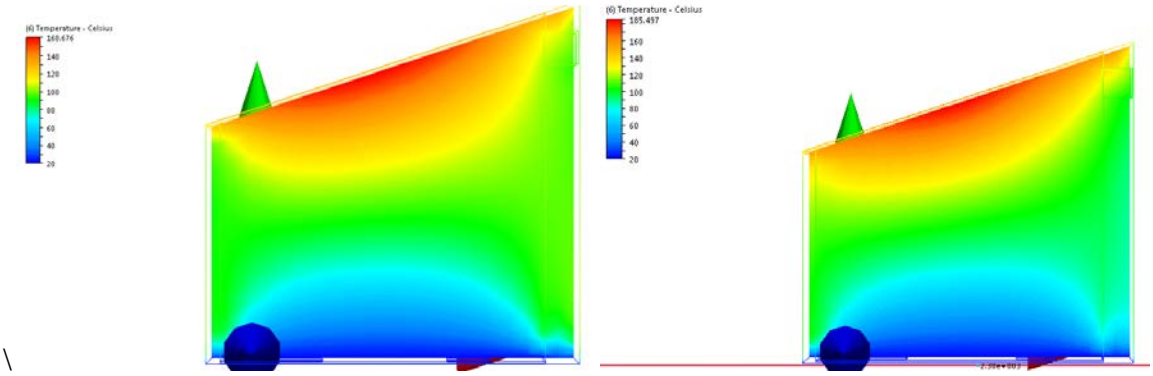

\

Figure 8: (a) Solar Heated at 1pm (b) Solar Heated at 2pm

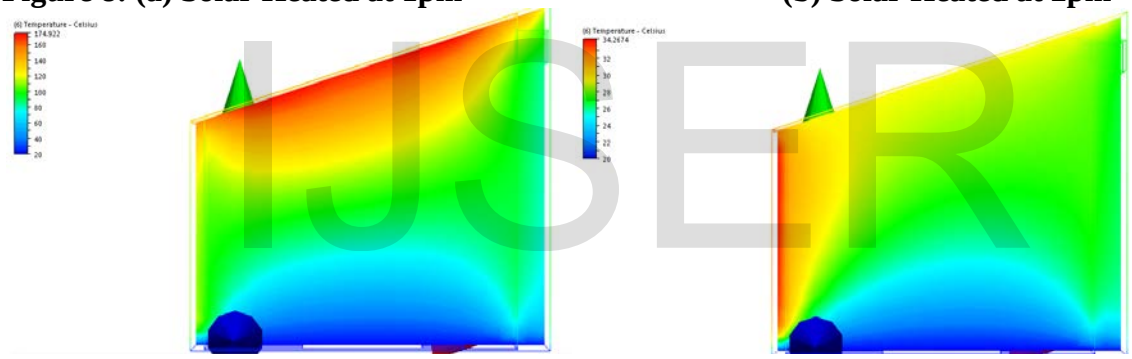

Figure 9: (a) Solar Heated at 3pm (b) Solar heated at 7pm

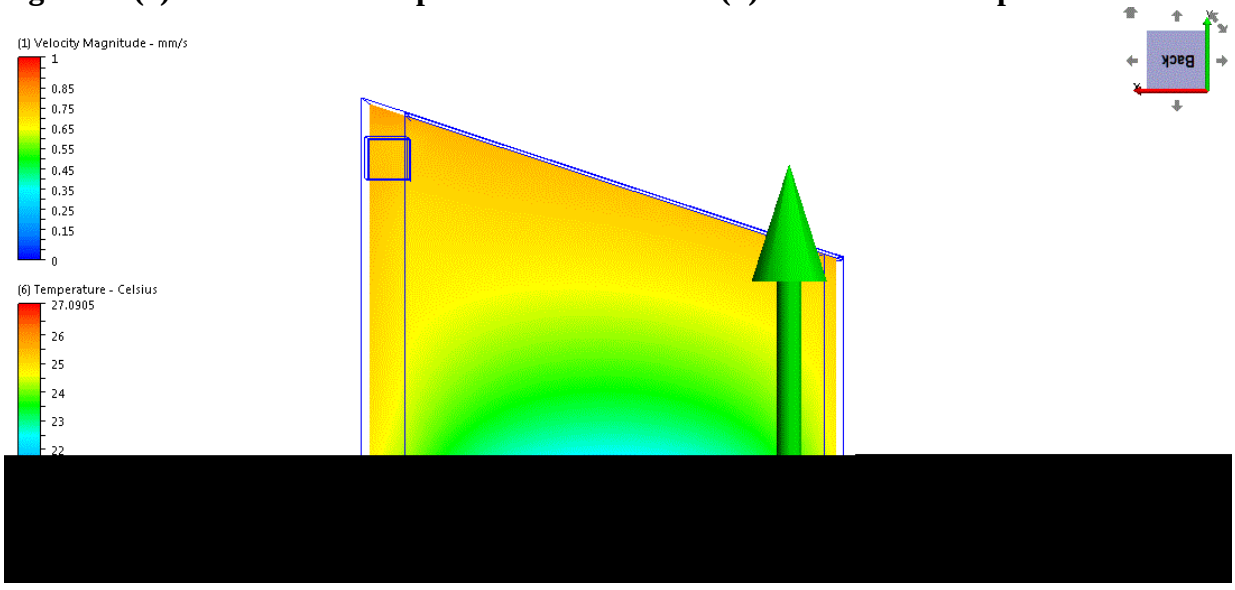

Figure 10: Solar Heated at 7am

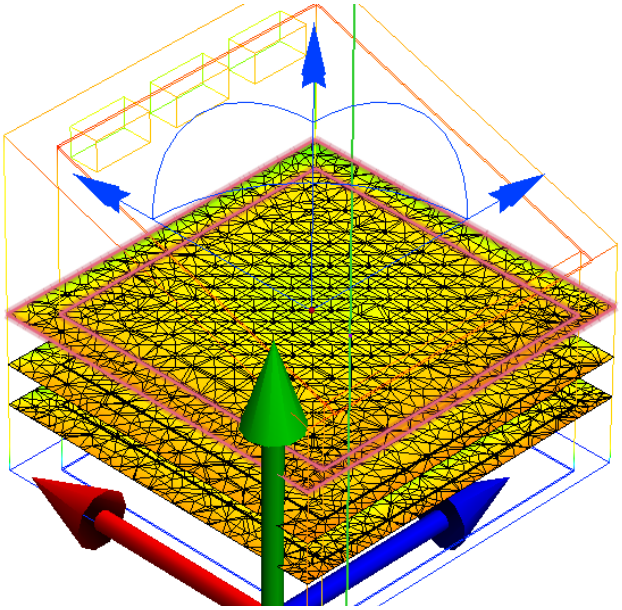

Figure 11: Temperature Distribution along the Planes under Solar Mode

3.4 Statistical Comparison of Simulated Results with the Experimental Results

The results of the experiment were compared with simulated results using Analysis of Variance (ANOVA) to know if there is a significant difference between the two results. The result presented in table 1 shows the summary of the pre-set level of significance for each of the parameters compared. The p-value obtained are 0.051, 0.062 and 0.763 which are higher than $\alpha = 0.01$ and 0.05. The result shows that none of the parameters varied significantly at $\alpha = 0.05$. This suggests that simulation work can be used to other parameters that affect drying.

Table 1: ANOVA of Results of Simulation and Experiment

Parameters	F	P	Remark
Velocity	0.10	0.763	No significant difference because P value is greater than 0.05
Temperature	4.12	0.062	No significant difference because P value is greater than 0.05

4. CONCLUSION

The solar-biomass hybrid dryer was constructed and tested without trays and load. The temperature and air flow data collected during experiment was used to validate the simulation results. From the temperature and velocity profiles simulated, it is deduced that heat and mass

transfer by natural convection is more suitable for drying ginger with solar radiation. In the natural convection model, the thermal heat distribution in the drying chamber was uniformly distributed, suitable for drying the ginger. The uniform heat distribution at the center of the drying chamber with a range from 335.4K to 352.0K is sufficient for drying the ginger at a wet base of 12%. The heat distribution in the drying chamber was more homogeneous in the natural convection model. The value of velocity across the plane is approximately the same as the velocity obtained through the experiment which was between 0.2 and 0.28 m/s. The flow velocity is high mainly along the axis of the hole from the base.

REFERENCES

[1] Green, M.G.,(2001).”Solar Drying Technology for Food Preservation”. Gate Information Service. http://www.gtz.de/gate

[2] Aworh, O.C., and Egounlety, A.M., (2009). “Status of Food Science and Technology in West Africa”.http://www.worldfoodscience.org/cms/?pid=1004846.

[3] Karim, M.A. and Hawlader, M.N.A.,(2005). “Mathematical Modelling and Experimental Investigation of Tropical Fruits Drying” *Journal of Heat and Mass Transfer* Vol. 48 pp 4914–4925.

[4] El-Sebaii, A. A. and Shalaby, S.M. (2012). “Solar Drying of Agricultural Products: A Review.Renewable and Sustainable Energy Reviews”, vol. 16, pp 37 -43.

[5] Rahman, M.S., (1999). “Handbook of Food Preservation”, Marcel Dekker, Inc. New York.

[6] Jangam, S.V. and Mujumdar, A.S., (2010). “Basic Concepts and Definitions, in: *Drying of Foods, Vegetables and Fruits”* - Volume 1, Singapore.

[7] Sandeep, P., Satish, K.S., Sunil, Y., Asim, K.T. and Ravi, N., (2013). “Design, Construction and Testing of Solar Dryer with Roughened Surface Solar Air Heater”. International Journal of Innovative Research in Engineering & Science. Vol. 7, pp 7-17.

[8] Ekechukwu, O.V. and Norton, B., (1999). “Review of Solar-Energy Drying System II: An Overview of Solar Drying Technology. Energy Conversion & Management 40: pp 615-655.

[9] Forson,F.K., Nazha, M.A.A., Akuffo, F.O., and Rajakaruna, H. (2007). “Design of Mixed-Mode Natural Convection Solar Crop Dryers: Application of Principles and Rules of Thumb”, *Renewable Energy* Vol.32 pp2306–2319.

[10] Mohsin, A.S.M., Nasimul, I. M, Sayem, A.H.M. Rejwanur R. M., and Hossain, M. S. F. (2011). “Prospect & Future of Solar Dryer: Perspective Bangladesh”. *IACSIT International Journal of Engineering and Technology, Vol.3, No.2,*

[11] Ghaffari, A. and Mehdipour, R. (2015). "Modeling and Improving the Performance of Cabinet Solar Dryer using Computational Fluid Dynamics". Int. J. Food Eng.: 11(2): 157 - 172

[12] Prasad, J., and Vijay, V.K., (2005). "Experimental Studies on Drying of *Zingiber officinale*, *Curcuma longa L*. and *Tinospora cordifolia* in Solar-biomass Hybrid Dryer". *Renew Energy*. Vol. 30 pp2097–2109.

[13] Singh Chauhan, P., Kumar, A. and Tekasakul, P. (2015). "Applications of software in Solar Drying Systems: A Review. Renewable and sustainable Energy Reviews". 51:1326 – 1337

[14] Rigit, A., R., and Low, P. T., (2010). "Heat and Mass Transfer in a Solar Dryer with Biomass Backup Burner," *World Academy of Science, Engineering and Technology*, pp. 115-118.

[15] Dyah, W., Nelwan, L., O., Kamaruddin, A. and Indra, S., A., (2003). "Analysis of Temperature and Air Flow Distribution in Solar Dryer Using CFD," *IPB (Bogor Agricultural University)*, vol. 17, no. 1, pp 121-132.

[16] Mathioulakis, E., Karathanos, V., T., and Belessiotis, V., G., (1998). "Simulation of air movement in a dryer by computational fluid dynamics: Application for the drying of fruits," *Journal of Food Engineering*, vol. 36, no. 2, pp. 183-200.

[17] Maia, C.B., Ferreira, A. G., Cabezas-Gomez, L., Hanriot, S. M. and Martins, T. O., (2012). "Simulation of the Airflow Inside a Hybrid Dryer". IJRRAS vol. 10 no. 3 pp382-389.

[18] Bolaji, B.O., (2005). "Performance evaluation of a simple solar dryer for food preservation. Proc. 6th Ann. Engin. Conf. of School of Engineering and Engineering Technology", Minna, Nigeria, pp. 8-13.

[19] Autodesk Simulation CFD (2013). "Autodesk Simulation CFD help", Autodesk, Inc.